Green Tea Catechins Potentiate Triclosan Binding to Enoyl-ACP Reductase from *Plasmodium falciparum* (PfENR)

Shailendra Kumar Sharma,[†,‡] Prasanna Parasuraman,[†,‡] Gyanendra Kumar,[†] Namita Surolia,*[,§] and Avadhesha Surolia*[,†,||]

Molecular Biophysics Unit, Indian Institute of Science, Bangalore 560012, India, National Institute of Immunology, New Delhi 110067, India, and Molecular Biology and Genetics Unit, Jawaharlal Nehru Centre for Advanced Scientific Research, Bangalore 560064, India

Received October 4, 2006

We have investigated the mechanism of inhibition of enoyl-acyl carrier protein reductase of *Plasmodium falciparum* (PfENR) by triclosan in the presence of a few important catechins and related plant polyphenols. The examined flavonoids inhibited PfENR reversibly with K_i values in the nanomolar range, EGCG being the best with 79 ± 2.67 nM. The steady-state kinetics revealed time dependent inhibition of PfENR by triclosan, demonstrating that triclosan exhibited slow tight-binding kinetics with PfENR in the presence of these compounds. Additionally, all of them potentiated the binding of triclosan with PfENR by a two-step mechanism resulting in an overall inhibition constant of triclosan in the low picomolar concentration range. The high affinities of tea catechins and the potentiation of binding of triclosan in their presence are readily explained by molecular modeling studies. The enhancement in the potency of triclosan induced by these compounds holds great promise for the development of effective antimalarial therapy.

Introduction

Malaria is one of the most devastating diseases of the tropical countries.[1] *Plasmodium falciparum* causes the fatal kind of malaria, *viz.* cerebral malaria. Emergence of drug resistance in the malarial parasite to the commonly used antimalarials has further worsened the current situation. Hence, there is an urgent need to discover novel pathways exclusive to the parasite which could be exploited for developing antimalarial agents. In this context, the discovery of a bacterial kind of fatty acid synthesis pathway in *Plasmodium falciparum* has opened new avenues to develop novel antimalarials.[2,3]

In all living organisms fatty acids are synthesized by either type I or type II fatty acid synthase (FAS [a]). Type I or the associative type, in which a single large multifunctional protein contains all the essential domains required to complete the fatty acid biosynthesis, is present in eukaryotes and certain mycobacteria.[4] In the type II FAS (dissociative type of FAS) several discrete enzymes carry out specific reactions to accomplish fatty acid synthesis.[5] Type II FAS is present in prokaryotes, plants, and several protozoans including the malaria parasite.[2,3,5,6] The differences in the architectural organization of the FAS systems of the host and parasite can, therefore, be utilized for the development of novel antimalarials.[2,3,7,8]

In *Plasmodium falciparum* fatty acid biosynthesis takes place in a relict plastid, called the apicoplast.[9] All the enzymes of FAS are encoded by nuclear genes and are transported to the apicoplast by a bipartite signal sequence.[10] The fatty acid elongation cycle contains four iterative steps: decarboxylative condensation, NADPH dependent reduction, dehydration, and NADH dependent reduction.[4−6] The fourth step is carried out by enoyl-acyl carrier protein (ACP) reductase (ENR), which reduces the *trans*-2-enoyl bond of enoyl-ACP substrates to saturated acyl-ACPs and plays a deterministic role in completing the fatty acid elongation cycles.[11] ENR has been validated as a potential target for the development of new antibacterials[6,12] and antimalarials.[2,3] We have extensively studied PfENR at biochemical as well as the structural level and also worked out the mechanism of triclosan binding to it.[13−17]

Green tea extracts (GTE) have been used extensively for treating many diseases.[18,19] They contain a variety of secondary metabolites, mainly flavonoids called catechins, which include (−) epigallocatechin gallate (EGCG), (−) epicatechin gallate (ECG), (−) epigallocatechin (EGC), (−) epicatechin (EC), etc.[18−20] It is reported that 200 mL of green tea contains 140 mg EGCG, 65 mg EGC, 28 mg ECG, and 17 mg EC.[20] GTE shows several pharmacological effects ranging from neuroprotection,[21] protection from Duchenne muscular dystrophy,[22] and inhibition of angiogenesis[19,20,23,24] as well as MMP-7 to prevent cancer metastasis and invasion.[25] Also, GTE inhibits HIV-1 reverse transcriptase,[26] cycloxygenase,[27] telomerase,[28] squalene epoxidase,[29] type I fatty acid synthase,[30,31] and Ribonuclease A.[32] Among the constituents of GTE, EGCG is the most effective flavonoid for treating various types of cancers and is a powerful antioxidant.[19] Tea catechins also inhibit type II fatty acid biosynthesis in *E. coli* by inhibiting β-ketoacyl-ACP reductase and enoyl-ACP reductase with IC_{50} in the 5−15 μM range.[33] An earlier study on inhibition of chicken FAS I by EGCG suggested that it inhibits the reductase component, mostly β-ketoacyl ACP reductase (FabG) at 50 μM range with K_i of 47.8 μM. It was also stated that EGCG inhibited keto-reductase activity more potently than the enoyl-reductase activity.[30] In a separate study, on mammalian FAS nine of the fifteen flavonoids tested gave IC_{50} values in the range of 2−112 μM, and it was found that the flavonoids containing two hydroxyl groups in the B ring and 5-, 7-hydroxyl groups in the A ring together with a C-2,C-3 double bond in combinations were the most effective inhibitors.[31] Among the flavonoids tested, morin was the best with an IC_{50} value of 2.33 μM, and quercetin gave

* To whom correspondence should be addressed. (N.S.) Tel.: 91-80-22082820. Fax: 91-80-22082766. E-mail: surolia@jncasr.ac.in. (A.S.) Tel.: 91-11-26717102. Fax: 91-11-26717104. E-mail: surolia@nii.res.in.

† Indian Institute of Science.

‡ These authors contributed equally to the work.

§ Jawaharlal Nehru Centre for Advanced Scientific Research.

|| National Institute of Immunology.

[a] Abbreviations: FAS, fatty acid synthase; ACP, acyl carrier protein; PfENR, *Plasmodium falciparum* enoyl-ACP reductase; FabG, β-ketoacyl-ACP reductase; GTE, green tea extracts; EGCG, epigallocatechin gallate; EGC, epigallocatechin; ECG, epicatechin gallate; CG, catechin gallate; Pf; *Plasmodium falciparum*; Ec, *Escherichia coli*; K_i, dissociation constant; TCL, triclosan.

10.1021/jm061154d CCC: $37.00
Published on Web 01/31/2007

IC_{50} of 4.29 μM. The major GTE, EGCG, inhibited type II FAS more effectively than type I FAS.

Recently, we observed that the substrate-binding loop region in PfENR is ordered both for the binary (PfENR−NADH) as well as the ternary complex (PfENR−NAD^+−triclosan), but in EcENR the loop becomes ordered or stabilized only after the formation of ternary complex.[17] Hence, we expected that these catechins will bind more tightly to PfENR than EcENR in binary complex itself and perhaps potentiate the inhibitory activity of triclosan. With this hypothesis, in the present study we conducted detailed studies with three catechins (EGCG, ECG, and EGC) and two related plant polyphenols (quercetin and butein) on PfENR. Interestingly, out of the five compounds tested, three showed IC_{50} and K_i values in the nanomolar range, proving that they are far better inhibitors of PfENR than its *E. coli* counterpart. We also show that the binding of these flavonoids is reversible in nature. What is more, they potentiate triclosan binding to PfENR at levels not observed with NAD^+,[14] bringing the overall inhibition constant of triclosan in the picomolar range (overall inhibition constant $K_i^* = 1.9 \pm 0.46$ pM). We provide an explanation for the higher inhibitory activity of the tea catechins and polyphenols toward PfENR as compared to that of EcENR and propose that EGCG in conjugation or in combination with triclosan can be used for developing more effective antimalarials.

Results and Discussion

"Better to be deprived of food for three days than tea for one" (an ancient Chinese proverb). This proverb reflects the importance of tea in daily life, and indeed the Chinese have harnessed the medicinal values of green tea for the past 4000 years.[18] Rock et al. studied the activity of a large number of tea catechins and plant polyphenols against various enzymes of type II fatty acid synthase (FAS) of *E. coli*.[33] It was shown that these compounds inhibited the reductase steps (FabG and FabI) of FAS II, and kinetic analysis indicated that these compounds interfere with the cofactor-binding sites of the reductases (FabG and FabI). β-Ketoacyl ACP synthase III (FabH) was also inhibited to some extent. The structure−activity relationship pointed out that the galloyl moiety of the catechins was absolutely necessary for EcENR/EcFabG inhibition. Two hydroxyphenyl rings connected by a two to three carbon linker was the fundamental requirement for their inhibitory effect.[33] Docking studies reported here provide an explanation for the importance of the galloyl moiety in the inhibitory activity of catechins. While this manuscript was under preparation a preliminary report describing inhibition by a miscellany of flavonoids and tea catechins against three of the *Plasmodium falciparum* enzymes (PfFabG, PfFabZ, and PfENR) appeared. The results for the IC_{50} and K_i values for the compounds common between our study and that of Deniz et al.[34] for PfENR are broadly in a similar range but differed in the kinetic mechanism, and also our main focus is on the potentiation of the inhibitory activity of triclosan by triclosan−PfENR−catechin ternary complex formation, which was not explored by Deniz et al.[34]

We had earlier analyzed the substrate-binding loops of several enoyl-ACP reductases in detail. PfENR differs significantly from other enoyl-ACP reductases in the substrate-binding loop conformation.[17] Comparison of the interactions of NAD^+ in binary and ternary complexes of PfENR and EcENR clearly indicate that in PfENR all five hydrogen bonds are conserved in the binary as well as in the ternary complex, while in the case of EcENR only one hydrogen bond is conserved in the binary complex against five in the ternary complex. So, in the case of a binary complex of PfENR, the loop is well ordered and has a closed conformation in close proximity to the binding site, making the active site "preformed" while in EcENR this loop is disordered and is only stabilized in the ternary complex.[17] As the catechins have multiple hydroxyl groups, they may make many more hydrogen bonds and other interactions with the substrate-binding loop of PfENR, making it even more ordered and stable.

For the sake of convenience and to avoid confusion, we will refer to all five compounds collectively as flavonoids. Further, EGCG has been treated as the representative compound of the five flavonoids used, and the data is discussed throughout mostly in the context of EGCG. For the remaining four compounds, figures are provided as Supporting Information.

Inhibition of PfENR by Tea Catechins and Polyphenols. Three of the tea catechins (EGCG, EGC, ECG) and two polyphenols (quercetin and butein), which gave IC_{50}s in the range of 5 to 30 μM for the *E. coli* ENR reported recently, were selected for the present study.[33] Among the five compounds tested, EGCG was the most potent ($IC_{50} = 250 \pm 6.2$ nM) inhibitor of PfENR (Figure 1a). The IC_{50} values of other compounds are shown in Table 1. Among the two polyphenols tested, quercetin gave an IC_{50} value of 2.5 ± 0.078 μM and butein 12.5 ± 0.67 μM. In comparison to the reported data on the *E. coli* counterpart[33] all these compounds showed improved IC_{50} values (Table 1).

Kinetics of Inhibition by Tea Catechins and Polyphenols. Kinetic parameters for all five flavonoids were determined individually against cofactor NADH and the substrate analogue crotonoyl-CoA, respectively. Earlier, it was shown that EGCG gave competitive kinetics against NADH with EcENR.[33] In the case of PfENR also, all five compounds showed competitive kinetics with NADH (Figure 1b and Supporting Information Figure 1). Their K_i values are shown in Table 2. With respect to the substrate analogue, crotonoyl-CoA, these compounds followed uncompetitive kinetics (Figure 1c and Supporting Information Figure 2). The K_i values of the individual compounds were calculated from the Dixon plot.[35] EGCG was the best compound with K_i value of 79.0 ± 2.67 nM, and the least effective compound was butein with K_i value of 2.97 ± 0.077 μM against crotonoyl-CoA. For the other flavonoids, K_i values against crotonoyl-CoA are given in Table 2. Analysis of the kinetic data clearly shows that EGCG along with the other flavonoids competes with NADH for binding to PfENR and inhibits its activity by preventing the binding of NADH. On the other hand, uncompetitive kinetics with respect to crotonoyl-CoA shows that crotonoyl-CoA somehow facilitates the binding of catechins. Notably, such a potentiation of the interactions of catechins by the substrate for other enzymes has not been observed earlier.

Analysis of Potency Assay. Binding of triclosan to both PfENR and EcENR is potentiated by NAD^+.[14,36,37] The competitive kinetics of tea catechins and polyphenols with PfENR with respect to NADH tempted us to investigate whether these compounds can mimic the effect of NAD^+ and potentiate triclosan binding to PfENR. The effect of flavonoids on triclosan binding was judged by the potency assay as described in the methods. From Figure 2, it is clear that the control reaction showed a linear mode of NAD^+ accumulation with respect to time (curve "a"), and addition of 150 nM triclosan to the reaction mixture impeded the rate of the reaction in a gradual manner (curve "b"). The onset of inhibition was faster when tea catechin (EGCG) was added along with triclosan (curve "c"). Incubation

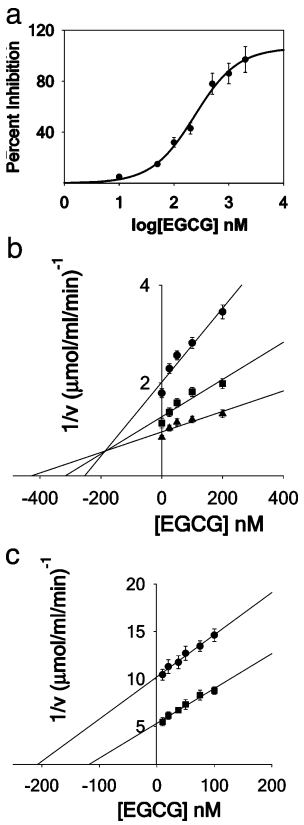

Figure 1. a. Inhibition of PfENR by EGCG. PfENR activity was determined in the presence of various concentrations of EGCG (10 nM to 2 μM). The percent inhibition was calculated from the residual PfENR activity and was plotted against log [EGCG] used. The sigmoidal curve indicates the best fit for the data, and the IC_{50} value was calculated from the graph. b. Inhibition kinetics of EGCG with respect to NADH. The effect of NADH on EGCG inhibition was determined using a Dixon plot. PfENR (30 nM) was assayed in presence of 200 μM crotonoyl CoA, 250 nM EGCG, and 50 μM [●], 100 μM [■], and 200 μM [▲] of NADH. The K_i of EGCG was calculated from the *X*-intercept using the equation for competitive kinetics. c. Inhibition kinetics of EGCG with respect to crotonoyl CoA. Here PfENR was assayed at two fixed concentrations, 100 μM [●] and 200 μM [■], of crotonoyl CoA in presence of 250 nM of EGCG and 100 μM of NADH. The K_i was calculated from the *X*-intercept of the Dixon plot, assuming uncompetitive kinetics.

of EGCG and triclosan for 30 min with PfENR further hastened the onset of inhibition (curve 'd"). Thus, the potency assay indicated that EGCG promoted the binding of triclosan to PfENR. It also hinted that triclosan behaved as a slow tight-binding inhibitor in the presence of EGCG.

Kinetic Behavior of Tea Catechins and Polyphenols in Conjugation with Triclosan. We further explored the effect of individual flavonoids on the dissociation constant of triclosan with PfENR and *vice-versa*. In the presence of NAD^+, K_i of 53 nM for triclosan with PfENR was calculated by Dixon plot.[14] In the presence of EGCG the K_i of triclosan came down to 1.0 $\pm$ 0.087 nM and followed uncompetitive kinetics (Figure 3a). All the compounds tested potentiated the binding of triclosan to PfENR (Table 2 and Supporting Information Figure 3).

Whether triclosan could also potentiate inhibition of PfENR by these flavonoids was then examined and K_i for each catechin was determined in the presence of triclosan. In this case also uncompetitive kinetics was observed (Figure 3b). The data showed a marked improvement in the K_i values of each flavonoids. As a model compound, the K_i of EGCG was improved by a factor of 10 and was calculated to be 8.0 $\pm$ 0.56 nM in the presence of triclosan whereas it was 79.0 $\pm$ 2.67 nM in the absence of triclosan. For the rest of the compounds also, the potencies were enhanced by triclosan (Table 2 and Supporting Information Figure 4).

Table 1. Comparison of IC_{50} Values of Different Selected Catechins on PfENR and EcENR.[33] EGCG Gave the Best Result on PfENR with an 250 nM IC_{50} Value

Tea extracts	Structure	IC_{50} [µM] with PfENR	IC_{50} [µM] values with EcENR
EGCG	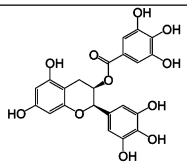	0.250 ± 0.0062	15
ECG	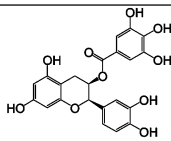	0.500 ± 0.016	10
EGC	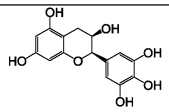	7.0 ± 0.085	>100
Quercetin	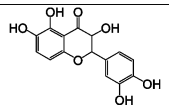	2.5 ± 0.078	20
Butein	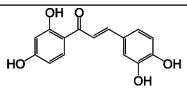	12.5 ± 0.67	30

Binding of [^{3}H]EGCG with PfENR. To confirm the above kinetic data, direct binding experiments of triclosan and EGCG with PfENR were designed using tritiated EGCG. Binding of [^{3}H]EGCG was conducted with PfENR in the absence as well as in the presence of triclosan. The binding of [^{3}H]EGCG to PfENR followed saturation kinetics (Figure 4a). The dissociation constant was calculated by saturation kinetics (eq 2a) and also by Scatchard plot[38] (eq 2b) (inset of Figure 4a), which gave the values of 438 $\pm$ 8.2 nM and 512 $\pm$ 28.78 nM, respectively. We then calculated the dissociation constant of EGCG in the presence of 10 μM triclosan. As can be seen from the gel filtration profile (Figure 4b), there is a noticeable increase in the counts of bound [^{3}H]EGCG to PfENR in the presence of triclosan. The counts of bound [^{3}H]EGCG increased from ~6000 cpm to ~18500 cpm in the presence of 10 μM of triclosan; this clearly indicated that triclosan potentiates the binding of EGCG to PfENR. The K_d calculated by saturation kinetics (Figure 4c) and Scatchard plot (inset of Figure 4c) was 89 $\pm$ 2.3 nM and 77.6 $\pm$ 5.3 nM, respectively. Finally, the binding constant of triclosan was determined at fixed concentration of [^{3}H]EGCG (1 μM) and variable triclosan concentration which also followed saturation kinetics (Figure 4d). The association constant of triclosan was determined to be 22.18 $\pm$ 1.7 μM^{-1} by saturation kinetics and 14 $\pm$ 0.77 μM^{-1} by double reciprocal plot (inset of Figure 4d). The dissociation constants were 45.1 $\pm$ 8 nM and 71 $\pm$ 4.3 nM, respectively.

The radiolabel binding results showed marked improvement in the K_d value of [^{3}H]EGCG in the presence of triclosan. The K_d value came down from 438 nM to 89 nM reflecting almost 5 times better affinity of EGCG in the presence of triclosan. From the above binding data it became evident that the presence

Table 2. Comparison of Detail Kinetic Parameters of the Tea Catechins by Spectrophotometric (Dixon Plot) and Fluorescence Titration Studies

tea catechin s	K_i w.r.t.[a] NADH [μM]	K_i w.r.t. crotonoyl-CoA [μM]	K_i of TCL [nM]	K_i in presence of TCL [nM]	K_i of TCL by fluorescence quenching [nM]
EGCG	0.186 ± 0.00798	0.079 ± 0.00267	1.0 ± 0.087	8.0 ± 0.56	7.29 ± 1.02
ECG	0.291 ± 0.0076	0.102 ± 0.0046	8.0 ± 0.084	16.0 ± 0.45	28.31 ± 5.74
EGC	3.75 ± 0.054	2.0 ± 0.078	8.25 ± 0.081	17.56 ± 0.67	52.71 ± 8.61
quercetin	1.09 ± 0.089	0.473 ± 0.011	10 ± 0.069	22.0 ± 0.85	30.54 ± 7.62
butein	5.5 ± 0.1	2.97 ± 0.077	13.72 ± 0.42	14.0 ± 0.57	71.02 ± 9.67

[a] w.r.t.: with respect to.

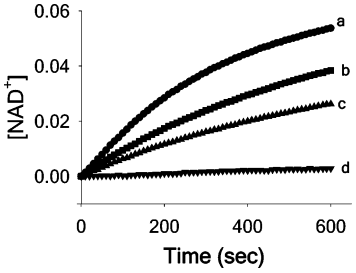

Figure 2. Slow onset of inhibition by triclosan in the presence of EGCG. The potency assay shows the slow onset of inhibition by triclosan. Curve "a" is the control reaction without EGCG and triclosan, curve "b" is inhibition reaction in presence of 150 nM triclosan, curve "c" depicts the onset of inhibition in the presence of 250 nM EGCG and 150 nM triclosan without preincubation, and curve "d" shows further potentiation of inhibition when EGCG and triclosan were preincubated with PfENR for 30 min. The Y-axis of the plot represents the production of NAD^+ in mM concentration with respect to time (in sec., X-axis).

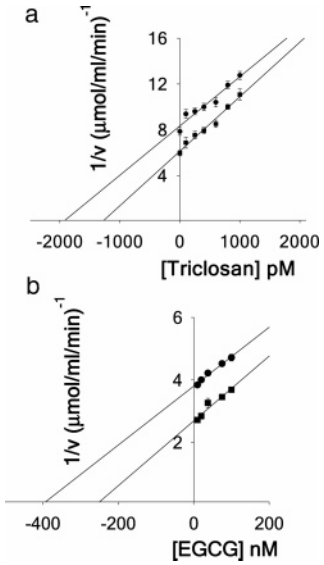

Figure 3. a. Effect of EGCG on the inhibition of PfENR by triclosan. Inhibition assay of various concentrations of triclosan in the presence of 50 nM [●] and 100 nM [■] of EGCG was conducted to assess EGCG's effect on dissociation constant of triclosan. As seen in the Figure triclosan followed uncompetitive kinetics with respect to EGCG. The K_i of triclosan was calculated to be 1 nM from the *x*-intercept. b. Effect of triclosan on the inhibition of PfENR by EGCG. EGCG gave uncompetitive kinetics with respect to 50 nM [●] and 100 nM [■] of triclosan as can be seen from the Dixon plot. The K_i of EGCG was calculated to be 8.0 ± 0.56 nM in the presence of triclosan.

of triclosan promoted the binding of [^{3}H]EGCG to PfENR. We expect a similar effect on triclosan binding by EGCG to PfENR as already demonstrated by the kinetic data.

Reversible Binding of EGCG to PfENR. As can be seen from Figure 4e, NADH was able to displace bound [^{3}H]EGCG from the enzyme, and at 100 μM of NADH almost 91−93% [^{3}H]EGCG complexed with PfENR was removed from the enzyme. The nonlinear regression analysis of the binding data gave a sigmoidal fit, and the EC_{50} of NADH (effective concentration of NADH to remove 50% of bound [^{3}H]EGCG) calculated from the fit was 15.6 ± 1.8 μM (inset of Figure 4e). These results corroborate our kinetic data, revealing that EGCG competes with NADH for binding to PfENR and also that binding of EGCG to PfENR is reversible and not covalent. Another line of evidence for reversible binding of EGCG to PfENR comes from the treatment of PFENR−[^{3}H]EGCG complex with 6 M guanidium hydrocholoride. After guanidium hydrocholoride treatment, less than 9% of [^{3}H]EGCG was retained with the denatured PfENR on the PVDF membrane (Figure 4f) and most of the (∼91−94%) dislodged triatiated EGCG was recovered in the filtrate, attesting to the noncovalent nature of complex formation between the enzyme and the flavonoids.

Detailed Analysis of the Progress Curves of Triclosan Inhibition in Presence of Tea Catechins and Polyphenols. Examination of the progress curves of inhibition by triclosan in the presence of different flavonoids yielded a similar pattern. The control reaction was set up with individual catechins and polyphenols without triclosan, and the rest of the reactions contained triclosan from 0 to 700 nM. From the progress curves (Figure 5 and Supporting Information Figure 5), it can be stated that for each concentration of triclosan the initial and steady-state velocities decrease exponentially with time and at higher triclosan concentrations the steady-state is reached rapidly but with a decrease in steady-state velocity (v_s). This implies that in the presence of flavonoids, triclosan interacts with the PfENR−flavonoid complex rapidly to form an initial complex and then slowly converts into a stronger PfENR−flavonoid−triclosan complex (mechanism 2).

The individual progress curves were analyzed by eq 3a, from which a series of k_{obs} values were determined for each concentration of triclosan for each flavonoid. The determined k_{obs} values were plotted against respective triclosan concentrations using eq 4 which resulted in a hyperbolic curve (Figure 6 and Supporting Information Figure 6). The hyperbolic curve is diagnostic of a two-phase binding behavior of the inhibitor[39,40] and thus proves that triclosan followed biphasic nature of binding reflecting slow, tight binding behavior with PfENR in the presence of EGCG and other flavonoids. The first phase consists of rapid formation of weak ternary complex of PfENR−TCL−EGCG (EI, in mechanism 2) which slowly isomerizes into a more stable ternary complex (EI^* in mechanism 2).

Determination of k_{off} or k_6 and k_{on} or k_5 for Triclosan in the Presence of Tea Catechins and Polyphenols. Dissociation rate constants for triclosan in the presence of tea catechins and polyphenols (k_6) were calculated from the dilution assay, where the dissociation of triclosan was monitored by the regain of activity of PfENR after 1000-fold dilution as mentioned in the methods. k_6 was calculated directly by plotting the NAD^+ formed against time in eq 3a using nonlinear least-squares fit. Keeping EGCG as a model compound, the k_{off} or k_6 of triclosan in the presence of EGCG was calculated to be 1.6×10^{-5} ±

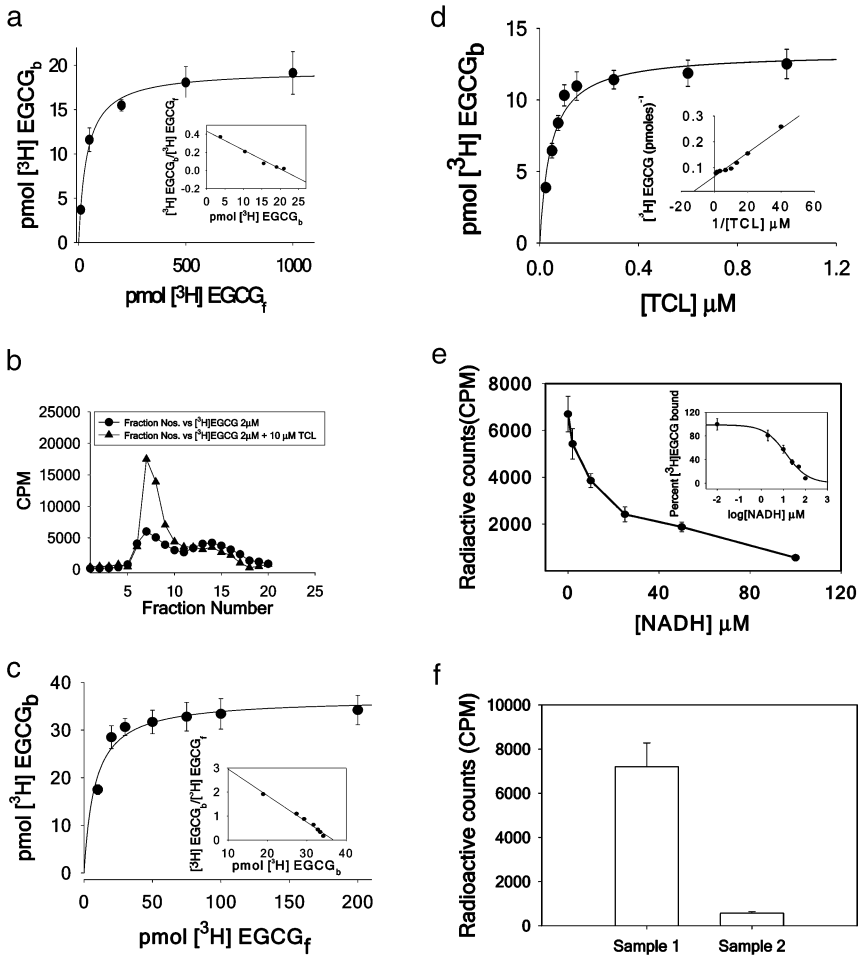

Figure 4. a. Binding of [^{3}H]EGCG to PfENR in the absence of triclosan. Binding of [^{3}H]EGCG to PfENR was analyzed by a filter-binding assay as described in Experimental Section and followed saturation kinetics with dissociation constant of 438 ± 8.2 nM, where [^{3}H]EGCG$_f$ and [^{3}H]-EGCG$_b$ are the bound and free concentration of [^{3}H]EGCG, respectively. The inset shows the Scatchard plot of the data. b. Gel filtration profile of [^{3}H]EGCG binding to PfENR. A 2 mL Sephadex G-25 column was used for gel filtration experiments with a void volume [V_o] of 680 μL. The gel filtration profile shows the plot of the fraction numbers versus radioactive count. Counts in the presence of 10 μM triclosan (TCL) [▲] the counts were dramatically increased near the void volume as can be seen from the gel filtration profile. c. Binding of [^{3}H]EGCG in the presence of triclosan. Binding was assessed using PVDF membranes as described in the text. In the presence of 10 μM TCL, [^{3}H]EGCG again showed saturation behavior. A nonlinear least-squares fit of the data yielded a K_i value of 89 ± 2.3 nM. The Scatchard plot for the data is shown in the inset which also gave a similar K_i value. d. Influence of triclosan on [^{3}H]EGCG binding. [^{3}H]EGCG showed saturation binding in the presence of increasing concentrations of TCL, giving a binding constant of 451 ± 7.7 nM. Double reciprocal plot of the same is shown in the inset. In all the above cases, saturation curves were plotted using eq 2a and the Scatchard plot by using eq 2b. e. Effect of NADH on the stability of the PfENR−[^{3}H]EGCG complex. A quantity of 8 μg of PfENR was incubated with 1 μM [^{3}H]EGCG for 20 min and then effect of NADH studied at increasing concentrations of NADH. NADH was able to displace bound [^{3}H]EGCG from the enzyme in a concentration dependent manner, proving that binding of EGCG is reversible and both (EGCG and NADH) compete for the same binding site on PfENR. Inset shows the nonlinear regression analysis of the above data. The best fit of the data gave a sigmoidal fit, and the EC_{50} value of NADH was calculated be 15.6 ± 1.8 μM. f. Effect of the denaturant, 6 M guanidium hydrochloride, on the dislodgment of [^{3}H]EGCG from the PfENR−[^{3}H]EGCG complex. A quantity of 8 μg of PfENR was incubated with 1 μM [^{3}H]EGCG for 20 min and then treated with 6 M guanidium hydrochloride for 3 h before taking the counts. The guanidium hydrochloride treatment showed a retention of only 6−9% of tritiated EGCG on the PVDF membranes. Sample 1 is the control reaction containing PfENR and [^{3}H]EGCG, and sample 2 contained control reaction mixture and 6 M guanidium hydrochloride.

0.078×10^{-5} s^{-1}. For all the other catechins the k_{off} data aresummarized in Table 3. The regain of activity after dilution indicates that triclosan and flavonoids do not make a covalent adduct with PfENR (Figure 7 and Supporting Information Figure 7) and thus supports the [^{3}H]EGCG binding data in the presence of NADH concluding that binding of EGCG with PfENR is reversible in nature. The very slow dissociation rate constant (k_6) reveals that the ternary complex [EI*] is highly stable and accounts for the extremely potent inhibition by triclosan in the presence of tea catechins and polyphenols.

The association rate constant or isomerization rate or onset of inhibition (k_5) of triclosan at fixed concentration of flavonoids were calculated from the progress curves discussed above generated after fitting the data to eq 3a. Progress curves gave the values of $k_{obs.}$ Values of k_5 were determined by fitting the values of k_{obs} with experimentally determined k_6 values in eq 4. The values of k_5 against each tea compound are given in Table 3. The low value of k_5 is responsible for the slow isomerization of the weak ternary complex into more stable ternary complex of PfENR−TCL−EGCG.

The overall inhibition constant (K_i*) of triclosan was calculated by eq 5 using the values of K_i, k_5, and k_6 of triclosan with respect to individual tea extracts and polyphenols (Table 3). Out of the five compounds tested, triclosan gave the best K_i* value of 1.9 ± 0.46 pM with EGCG. The overall inhibition

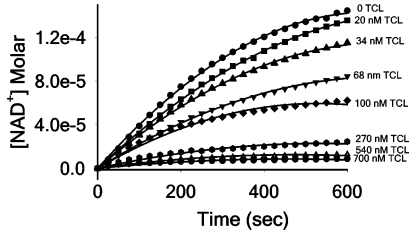

Figure 5. Progress curves. For each concentration of triclosan, a progress curve was generated using eq 3a. In the standard reaction mixture (as described in Experimental Section), a 100 nM EGCG solution was added which served as the control reaction. Triclosan was added to the control reaction at various concentrations [0−700 nM] as indicated in the figure.

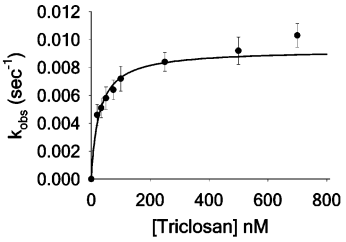

Figure 6. Dependence of PfENR inhibition on triclosan concentration in the presence of EGCG. The initial rate constant (k_{obs}) for each triclosan concentration added was calculated from the progress curves using eq 3a. The k_{obs} thus calculated and the respective Triclosan concentrations were fitted to eq 4, and the best fit gave a hyperbolic curve demonstrating a two-phase inhibition mechanism.

Table 3. Determination of the Overall Inhibition Constant of Triclosan in the Presence of Tea Catechins Using Steady-State Kinetics. Rate Constants, k_5, k_6, and K^* Values Were Determined Using eqs 3, 4, and 5, Respectively

tea extracts	isomerization rate constant [k_5] of triclosan, [10^{-3}] s^{-1}	dissociation rate constant [k_6] of TCL, [10^{-5}] s^{-1}	overall inhibition constant of TCL [K_i*] [pM]
EGCG	8.4 ± 0.24^a	1.6 ± 0.078^a	1.9 ± 0.46^a
	9.011 ± 0.6^b	11.31 ± 1.84^b	11.02 ± 2.48^b
EGC	5.4 ± 0.097^a	7.4 ± 0.68^a	109 ± 8.6^a
	18.23 ± 2.5^b	30.12 ± 6.4^b	206 ± 16.5^b
ECG	6.3 ± 0.135^a	4.1 ± 0.27^a	52.06 ± 3.56^a
	7.8 ± 0.6^b	20.01 ± 7.35^b	132.5 ± 17.7^b
quercetin	3.1 ± 0.0786^a	8.7 ± 0.334^a	280.6 ± 11.78^a
	11.5 ± 2.02^b	80.01 ± 14.6^b	892.3 ± 61.85^b
butein	2.1 ± 0.108^a	13.0 ± 0.809^a	798.33 ± 64.47^a
	11.28 ± 4.1^b	70.18 ± 20.3^b	800.5 ± 46.35^b

[a] k_6 value was obtained from the dilution assay method, k_5 value was determined by putting the value of k_6, k_{obs} (obtained from progress curve analysis), and K_i (obtained from the Dixon plot) in eq 4. The corresponding K_i^* was calculated using eq 5. [b] k_5 and k_6 values as determined from the plot of k_{obs} versus [triclosan].

constant (K_i^*) of triclosan in the presence of EGCG is roughly 50 times better than in the presence of NAD^+ where it is 96 pM.[14]

The values of kinetic constants varied when different methods were employed (Table 3). The value of overall inhibition constant (K_i^*) also varied accordingly. Depending upon the method used for calculating kinetic constants, the value of K_i^* varied from 1.9 to 11.02 pM. But in both the cases the data suggest the common theme that inhibition of PfENR by triclosan is potentiated by EGCG and other flavonoids examined.

Fluorescence Studies. We analyzed the triclosan binding to PfENR−flavonoid complexes by monitoring the rapid fluorescence decrease ($F_o - F$), at 340 nm after each addition of

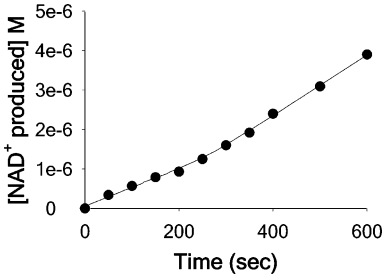

Figure 7. Dissociation rate constant (k_6) of the PfENR−triclosan−EGCG complex. PfENR was incubated with an equimolar quantity of triclosan and 10 μM EGCG solution for 30 min as described in Experimental Section. The reaction mixture was diluted 1000 times with competing NADH and crotonoyl CoA. Oxidation of NADH to NAD^+ was plotted against time. The data were analyzed by nonlinear regression using eq 3. k_6 of triclosan thus calculated was 1.6×10^{-5} s^{-1}.

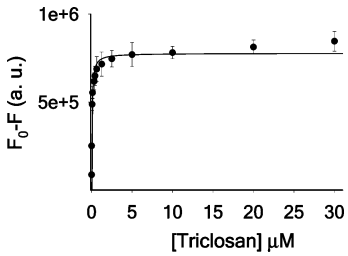

Figure 8. Effect of triclosan concentration on tryptophan fluorescence. A 5 μM PfENR solution preincubated with 100 nM EGCG was used in this study. triclosan was added sequentially from 0 to 30 μM. The fluorescence was measured at 25 °C. The samples were excited at 290 nm, and the emission was monitored at 340 nm. Change in fluorescence [$F_o - F$], after correcting for inner filter effect, was plotted against triclosan concentrations using eq 6. The best fit of the data yielded a hyperbolic curve.

triclosan (Figure 8 and Supporting Information Figure 8). The K_i of triclosan against each of the five flavonoids were calculated after fitting the data to eq 6. Before calculating K_i and k_5 from fluorescence data, the corrections for inner filter effect were made using eq 8. In the presence of EGCG, triclosan gave a K_i value of 7.29 ± 1.02 nM; the K_is for the rest of the compounds are shown in Table 2. For calculating k_5, the time course of fluorescence quenching for 30 min was monitored, resulting in a rapid fluorescence decrease for the initial phase followed by a slow decrease, which proves the binding to be a two-step mechanism (Figure 9). The initial rapid fluorescence decrease depicts the formation of the reversible PfENR−catechin−triclosan ternary complex, and the second phase is the slow conversion to the tight ternary complex. k_5 of triclosan in presence of EGCG calculated from the slow decrease of fluorescence using eq 7 was $0.0072 \pm 0.84 \times 10^{-5}$ s^{-1}. The data obtained from fluorescence studies are in agreement with the enzyme inhibition kinetics data.

Docking of Tea Catechins and Polyphenols with PfENR and EcENR. Docking studies with AutoDock show that tea catechins and flavonoids indeed occupy NAD^+ binding site (Figure 10a). Docking energies for all five flavonoids are summarized in Table 4. The main reason for the high affinities of these compounds for ENRs is the extensive hydrogen-bonding network involving their hydroxyl groups. Overall, the number of favorable interactions is more in the case of flavonoid−PfENR complex compared to the flavonoid−EcENR complex, accounting for the higher affinity of the flavonoids for PfENR (Table 5). As a model case we compared the interactions of

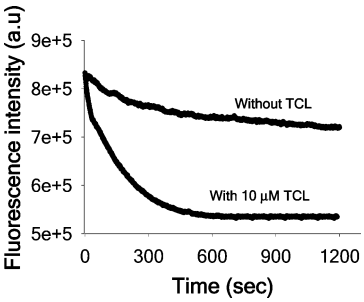

Figure 9. Time-dependent fluorescence quenching of PfENR by triclosan in the presence of EGCG. A 5 μM PfENR solution was incubated with 5 μM EGCG, and the time course of fluorescence quenching was followed for 20 min and served as a control reaction. The excitation and emission wavelength were set at 295 and 340 nm, respectively. To the control reaction was added 20 μM triclosan, and the time course of fluorescence decrease was monitored for 20 min. A rapid fall in fluorescence intensity suggests the quick formation of the PfENR−EGCG−triclosan ternary complex, which undergoes slow transition to the more stable ternary complex.

Table 4. Summary of Mean Docking Energies of the Catechins As Determined from Their Individual Binary Complexes with PfENR

tea extracts	mean docked energy [kcal/ mol]	IC_{50} values with PfENR
EGCG	−18.00	0.250 ± 0.062
ECG	−15.27	0.500 ± 0.016
EGC	−12.31	7.0 ± 0.085
quercetin	−12.01	12.5 ± 0.67
butein	−11.46	2.5 ± 0.078

EGCG with PfENR and EcENR. Cluster analysis of the docked conformations from 100 independent docking simulations was done with 1 Å rmsd. Though there were some individual conformations across the PfENR active-site, the most populated clusters with 20 and 9 conformations were found occupying the pocket where the adenine half of NAD^+ binds (Figure 10a). The spread of the entire ensemble of 100 conformers of EGCG examined for PfENR and EcENR are shown, respectively, in Supporting Information Figures 9a and 9b. The galloyl moiety plays a major role in the affinity of EGCG with both ENRs. It occupies the same pocket as the adenine ring of NAD^+ in the cofactor-binding site of the enzyme. Its phenol ring makes an aromatic stacking interaction with the side-chain Trp35 of PfENR similar to that of the adenine ring of NADH. It is also involved in hydrophobic interactions with Leu120. In the case of EcENR the galloyl moiety makes T-shaped aromatic interactions with Phe93.

The benzopyran moiety of EGCG occupies a cavity which otherwise accommodates the phosphate group of the adenine half of NAD^+ in both PfENR and EcENR. The hydrogen bonds are comparatively longer in the case of EcENR than those in the case of PfENR and hence weaker. As calculated from the LPC-CSU server, the benzopyran moiety contributes to most of the unfavorable contacts with the two enzymes. The number of such contacts is more in the case of EcENR compared to PfENR, as calculated from the LPC-CSU server. There is a striking difference in the interactions of the non-galloyl phenol ring with PfENR and EcENR. In the former it occupies the same space as occupied by the ribose and phosphate groups of the nicotine moiety of NAD^+, but in EcENR many conformations occupy the space which accommodates ribose of the adenine moiety of NAD^+, a flip of 180°, and it further extends in this pocket to make more interactions with the enzyme (Figure 10b).

Overall, the favorable interactions between EGCG and ENR are more, and unfavorable contacts significantly less, in the case

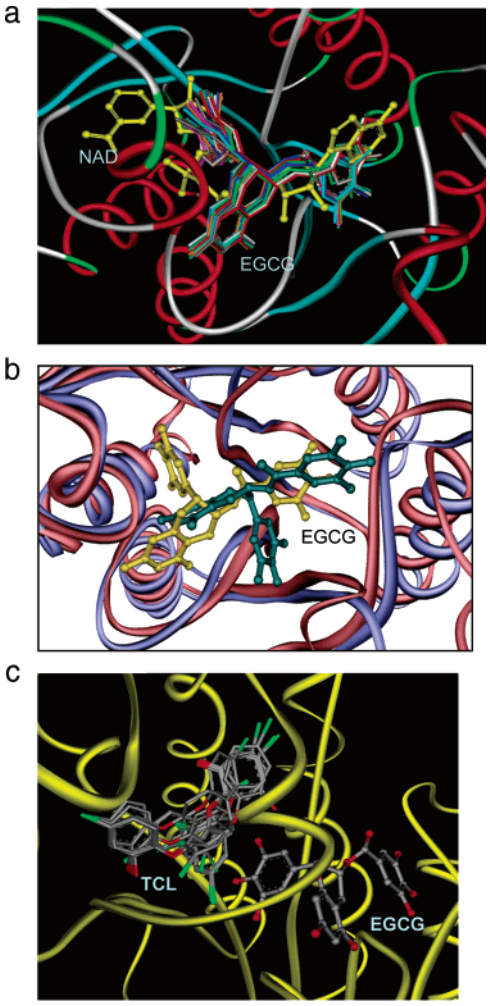

Figure 10. a. Ensemble of the docked conformations of the two biggest clusters (cluster sizes 20 and 9) from 100 docking runs of EGCG on PfENR. For the sake of clarity, not all 100 conformations are shown. PfENR is shown in ribbons, NADH as a reference in yellow balls and sticks, and EGCG conformations in sticks of different colors. b. EGCG−PfENR and EGCG−EcENR docked complexes superimposed on each other. To compare the two complexes, top conformations of biggest clusters in the respective complexes are shown. EGCG is represented as a ball and stick model and the enzyme in ribbons. PfENR is represented as brown ribbons with the corresponding EGCG colored in yellow, and EcENR is represented in blue ribbons with the corresponding EGCG colored in green. c. Ensemble of triclosan conformations docked with the PfENR−EGCG binary complex. EGCG is represented in balls and sticks, and triclosan conformations in sticks. PfENR is shown in ribbons. Atom colors; C in gray, O in red, N in blue, and Cl in green. Hydrogens are not shown for sake of clarity. Docking studies were performed using AutoDock program as detailed in the methods. The figures were generated using Weblab Viewerlite and rendered using POV-Ray.

of *P. falciparum* compared to *E. coli* (Table 5). This explains the higher affinity of EGCG for PfENR compared to EcENR.

Docking of Triclosan with the EGCG−PfENR Complex. Triclosan was docked with the binary complex of EGCG and PfENR to achieve the ternary complex. As mentioned in the above section, EGCG occupies the adenine binding pocket of the cofactor-binding site. Cluster analysis was performed for the docked conformations of triclosan from the 100 independent runs. The clusters with highest number of conformations lie in the pocket where the nicotinamide moiety of NAD^+ would bind otherwise. The biggest cluster had 51 conformations with a few smaller clusters. The ensemble of these conformations is shown

Table 5. Comparison of All the Stabilizing and Destabilizing Contacts Made by EGCG in Binary Complexes with PfENR and EcENR

contacts made in binary complexes	hydrogen bonds	hydrophobic contacts	aromatic−aromatic contacts	hydrophilic−hydrophobic contacts [destabilizing]	acceptor−acceptor [destabilizing]
ECGC-PfENR	27	21	10	19	2
ECGC-EcFabI	18	34	6	24	2

in Figure 10c, while the entire ensemble of 100 conformations of triclosan is shown in the Supporting Information Figure 9c. Stacking of the aromatic rings of triclosan and NAD^+ in the ternary complex of PfENR−NAD^+−triclosan plays a major role in the binding of triclosan;[15,41] similar stacking interactions are also observed between the phenyl rings of triclosan and non-galloyl phenyl ring of EGCG. This would contribute enormously in the formation of a strong PfENR−EGCG−triclosan ternary complex (Figure 10c). Rigorous molecular dynamics simulations on this docked ternary complex might shed more light on the formation of a stable ternary complex starting from an initial complex.

While both polyphenols and catechins are able to potentiate the affinity of triclosan by ternary complex formation to the same extent as NAD^+, the lower concentration of the former compound required to achieve the effect as compared to that required of NAD^+ is a favorable property which can be utilized for treating malaria and bacterial infection, which are dependent on Type II FAS for their growth. Moreover, the tea catechins and polyphenols exhibit their potentiation of triclosan at nanomolar concentrations but the concentration of NAD^+ required to potentiate the inhibitory activity of triclosan is in the high micromolar to millimolar range. At such a high concentration, its administration is likely to cause rearrangement in the metabolism itself. Administration of tea catechins and related polyphenols required to achieve the same effect is in the nanomolar to low micromolar range, and a much higher concentration of the same are tolerated by the host without any apparent side effect.

Conclusions

This study shows that certain medicinally important secondary metabolites found in the most commonly consumed beverage, tea, inhibit enoyl-ACP reductase (PfENR) of *Plasmodium falciparum* at nanomolar concentrations. These tea catechins and related polyphenols also inhibit mammalian FAS but with a K_i in the micromolar range, which is far greater than the *Plasmodium* counterpart. The vast difference in K_is of EGCG between the host and the parasite ENR underscores the significance of this study. We have also shown that flavonoids binding to PfENR are reversible in nature and they bind near the cofactor-binding site of PfENR. Most importantly, we have shown that the binding of triclosan is potentiated by tea catechins and *vice-versa* by steady-state kinetics and also by radiolabeled [^{3}H]-EGCG-binding experiments, bringing the overall inhibition constant of triclosan to less than 2 pM. The inhibition by triclosan followed a biphasic mode with a slow, tight-binding mechanism. Thus, the above findings suggest that these tea catechins and polyphenols, especially EGCG, can be used in the formulation of antimalarial therapy, either alone or in conjugation with triclosan as a combination drug. The only caveat for this assumption is that EGCG, the prime tea catechin, nonspecifically targets some other pathways in *E. coli* as well as humans. However, the fact that EGCG potentiates the binding of triclosan to PfENR and *vice-versa* suggests that the chances of EGCG inhibiting other pathways is minimized, as the major amount of EGCG is likely to be utilized by triclosan for making a stable ternary complex with PfENR. Another way to make the catechin molecules specific to PfENR is to chemically manipulate the essential galloyl scaffold of these catechins by rational drug design using the PfENR structure. The above findings hold great promise for the fight against malaria, as the tea catechins are nontoxic, inexpensive, and abundant in nature.

Experimental Section

Materials. Green tea catechins, butein, quercetin, crotonoyl-CoA, β-NADH, β-NAD^+, and all the PAGE reagents were purchased from Sigma-Aldrich, and kanamycin A and IPTG were purchased from Merck. Triclosan was a gift from Kumar Chemicals, Bangalore, India.

Overexpression of PfENR. Overexpression of PfENR was achieved essentially following the published protocol[13] with the only difference that all buffers contained 10% glycerol. Purity of the enzyme was checked by SDS-PAGE. Purified enzyme was stored in −20 °C at a concentration of 5 mg/mL till further use.

Assay of PfENR. Enzyme assays and inhibition studies were performed on a UV−vis spectrophotometer (Jasco) at 25 °C in 20 mM Tris/HCl and 150 mM NaCl, pH 7.4.[13,14] The standard reaction mixture of 100 μL contained 200 μM crotonoyl-CoA, 100 μM NADH, and 30 nM PfENR. All the inhibitors were dissolved in DMSO. 1% DMSO was used in the standard reaction mixture. The reaction proceeds by reduction of crotonoyl-CoA to butyryl-CoA with the oxidation of NADH to NAD^+ which is monitored at 340 nm ($\epsilon^{M}_{340} = 6220\ M^{-1}\ cm^{-1}$).

Determination of IC_{50} Values. IC_{50} values of the tea catechins and polyphenolic compounds for PfENR were determined by plotting the percent inhibition of PfENR at various concentrations of these compounds. In the standard reaction mixture mentioned above, various concentrations of EGCG or other catechins were added and the percent inhibition was calculated from the residual enzymatic activity. The percent activity thus calculated was plotted against log of concentration of the respective flavonoids. The data was analyzed by a nonlinear regression method.

Calculation of Dissociation Constants (K_i). The K_i of individual flavonoids were determined with respect to NADH and crotonoyl-CoA in separate experiments. With respect to NADH, data were collected against three fixed concentrations of NADH (50 μM, 100 μM, and 200 μM) while varying the catechin concentration from 1 nM to their respective IC_{50} values and keeping crotonoyl-CoA concentration fixed at 200 μM. For K_i with respect to crotonoyl-CoA, data were collected against two fixed concentrations of crotonoyl-CoA (100 μM and 200 μM) and catechin concentration was varied from 1 nM to the IC_{50} value, while NADH concentration was kept at 100 μM. All the data were analyzed by a Dixon plot.[35]

Potency Assay. Potency assays for triclosan inhibition of PfENR were designed as described earlier.[14,36] The effect of addition of tea catechins and polyphenols (IC_{50} values) without preincubation and with 30 min preincubation with triclosan (150 nM) on the activity of PfENR (30 nM) were studied. The formation of NAD^+ was monitored at 340 nm after the addition of 200 μM crotonoyl-CoA and 100 μM NADH. The control reaction was set up without the addition of triclosan with tea catechins and 1% DMSO. The accumulation of the product [NAD^+] in each case was plotted against time.

Determination of K_i of Triclosan in Presence of the Tea Catechins and Polyphenols. The K_i of triclosan with respect to various tea extracts and polyphenols was also determined by Dixon plot.[35] At two different catechin concentrations (around IC_{50} value of individual catechins), the triclosan concentration was varied from 0 to 700 nM. Likewise, the K_i of each flavonoid was determined at two fixed concentration of triclosan (50 nM and 100 nM) while

varying the concentration of the individual flavonoids. All the data of individual experiments were repeated thrice, and the mean value was taken for data analysis. The K_i values were determined for each experiment from the *X*-intercept of the Dixon plot.[35]

Analysis of [^{3}H]EGCG Binding to PfENR. Binding studies of [^{3}H]EGCG were carried out with PfENR in the absence and presence of triclosan employing two methods, gel filtration chromatography and filter-binding assay. Binding studies were carried out at 25 °C for 20 min in 20 mM Tris, 150 mM NaCl, pH 7.4, containing 1 μM [^{3}H]EGCG (specific activity 5 Ci/ mmol), varying concentration of triclosan, 1% DMSO, and 8 μg of PfENR in 50 μL of volume. Briefly, for gel filtration chromatography, a 2 mL Sephadex G-25 column was packed and equilibrated with the reaction buffer. For each run, 50 μL of the reaction mixture was loaded and 20 fractions of 100 μL were collected at 0.25 mL/ min flow rate. All the fractions were spotted on Whatman 3 filter paper and dried before taking the counts. In the filter-binding assay method, the reaction mixtures were directly applied on the activated polyvinylidene difluoride (PVDF) membrane fixed in a filtration assembly. The filters were washed with 200 μL of reaction buffer and dried. Dried filters were transferred to vials containing 5 mL scintillation fluid, and the radioactivity was measured using a Hewlett-Packard liquid scintillation counter.

To check the binding of [^{3}H]EGCG alone, five concentrations of [^{3}H]EGCG (0.1 to 10 μM), as indicated in Figure 4a, were taken. The concentration of [^{3}H]EGCG (bound) was plotted against [^{3}H]-EGCG (free) to get the binding constant. To determine the binding constant of EGCG in the presence of triclosan, the above experiments were repeated in the presence of 10 μM triclosan (Figure 4c). Finally, to determine the binding constant of triclosan in the presence of EGCG, various concentrations of triclosan were used (25 nM to 1 μM as indicated in Figure 4d) with 1 μM [^{3}H]EGCG. The binding constants for the above experiments were determined from saturation plots and also by a Scatchard plot or double reciprocal plot using eqs 2a and 2b described under Evaluation of the Kinetic Data.

Reversible Binding of [3H]EGCG to PfENR. The effect of NADH on the stability of PfENR−[^{3}H]EGCG complex was studied employing the filter-binding assay. Binding studies were carried out at 25 °C in 20 mM Tris, 150 mM NaCl, pH 7.4. PfENR (8 μg) was incubated with 1.0 μM [^{3}H]EGCG (specific activity 5 Ci/mmol) for 20 min and then varying concentrations of NADH (1−100 μM) were added into 50 μL reaction volumes. The reaction mixture was spotted on PVDF membranes and washed with 200 μL of reaction buffer and dried. The counts were taken as described above. The data was analyzed by linear as well as nonlinear regression methods.

Whether [^{3}H]EGCG forms covalent or noncovalent complexes with the enzyme was also examined by subjecting the PfENR−[^{3}H]EGCG complex to treatment with 6 M guanidinimum hydrochloride. PfENR (8 μg) was incubated with 1.0 μM [^{3}H]EGCG (specific activity 5 Ci/mmol) for 20 min and then incubated with 6 M guanidium hydrochloride for 3 h at 25 °C followed by spotting the denatured complex on PVDF membranes. Subsequently, the sample was washed with 200 μL of the reaction mixture buffer followed by drying and counting for [^{3}H]EGCG retained on the membranes and in the wash as described above. The control reaction contained all the above-mentioned components except 6 M guanidium hydrochloride and was incubated for the same time period before taking the counts.

Determination of Isomerization Rate or Association Rate (k_5 or k_{on}) and Dissociation Rate Constants (k_6 or k_{off}) of Triclosan in the Presence of Flavonoids. The association rate constants (k_5) of triclosan with PfENR in the presence of different tea catechins and polyphenols were determined by monitoring the onset of inhibition in the enzyme reactions, which contained 100 μM NADH, 200 μM crotonoyl-CoA, individual flavonoids at their respective IC_{50} values, and various concentrations of triclosan (0 to 700 nM). The reaction was started by the addition of 30 nM of PfENR. For each concentration of triclosan, the formation of NAD^+ was plotted against time by nonlinear regression method using eq 3a discussed below to get k_{obs} for each concentration of triclosan used. The k_{obs} values are fitted to eq 4 along with K_i and k_6 values to get the value of k_5.

The dissociation rate constants (k_6) for triclosan for various flavonid−PfENR complexes were determined by dilution method. PfENR (15 μM) was incubated with 15 μM triclosan and 10 μM of individual tea catechins and polyphenols for 30 min. The reaction was started with 1000-fold dilution of the PfENR−triclosan−EGCG ternary complex with buffer containing competing NADH and crotonoyl-CoA to a final concentration of 100 μM and 250 μM, respectively. The reaction was monitored at 340 nm, and the formation of (NAD^+) was plotted as a function of time using eq 3a to get the dissociation constant by nonlinear regression analysis of the data.

Calculation of Overall Inhibition Constant (K_i*). After the determination of K_i, k_5, and k_6 values, overall inhibition constant is calculated by putting their values into eq 5.

Evaluation of the Kinetic Data. Initial rate constants were determined using a Dixon plot,[35] assuming the reaction to be competitive for tea catechins against NADH and uncompetitive for tea catechins against triclosan. The data were plotted using the following Dixon equations for competitive and uncompetitive kinetics, respectively.

$$\frac{1}{v} = \frac{K_m \times [I]}{V_{max} \times K_i \times [S]} + \frac{1}{V_{max}\left(1 + \frac{K_m}{[S]}\right)} \quad (1a)$$

$$\frac{1}{v} = \frac{[I]}{V_{max} \times K_i} + \frac{1}{V_{max}\left(1 + \frac{K_m}{[S]}\right)} \quad (1b)$$

where K_m is the Michaelis constant, V_{max} is the maximal catalytic rate at saturating substrate concentration [*S*], [*I*] is the concentration of inhibitor, and K_i is the dissociation constant of the inhibitor (eq 1a is for competitive kinetics and 1b is for uncompetitive kinetics).

The binding of [^{3}H]EGCG to PfENR was analyzed by saturation and Scatchard plot[38] using eqs 2a and 2b, respectively.

$$[S]_b = \frac{[S]_{bmax} \times [S]_f}{K_d + [S]_f} \quad (2a)$$

where $[S]_b$ is the bound, $[S]_f$ is free, and $[S]_{bmax}$ is the maximum binding of the ligand being analyzed, and K_d is the dissociation constant.

$$\frac{[S]_b}{[S]_f} = -\frac{1}{K_d[S]_b} + \frac{n[E]_t}{K_d} \quad (2b)$$

where *n* is the number of identical and independent ligand-binding sites per molecule of enzyme, and $[E]_t$ is the total concentration of enzyme.

Time dependent reversible inhibition can be described by any of the two mechanisms described below.[39,40] In mechanism 1, the inhibitor and enzyme react with each other in a single-step bimolecular reaction to form an effective enzyme−inhibitor complex. This kinetics results either from slow association or sometimes slow dissociation of the inhibitor.

$$E + I \underset{k_4}{\overset{k_3}{\leftrightarrow}} EI \quad \text{(mechanism 1)}$$

In mechanism 2, the inhibition takes place in two steps, in the first step the enzyme binds rapidly with the inhibitor forming EI complex which, then slowly isomerizes to a more stable and effective EI* complex

$$E + I \underset{k_4}{\overset{k_3}{\leftrightarrow}} EI \underset{k_6}{\overset{k_5}{\leftrightarrow}} EI^* \quad \text{(mechanism 2)}$$

In both the mechanisms it is presumed that the slow-binding inhibition step is reversible.

The biphasic progress curves which are typical for slow, tight-binding inhibition were fitted to eq 3a[14,39,40,42] using a nonlinear least-squares fitting procedure.

$$P = v_s \times t + \frac{(v_o - v_s)[1 - \exp(-k_{obs} \times t)]}{k_{obs}} + C \qquad (3a)$$

where P is the concentration of the product formed at any given time t, v_o is the initial velocity, v_s is the final steady-state velocity, k_{obs} is the apparent first-order rate constant for the establishment of the final steady-state equilibrium, and C is a constant, nonzero Y-intercept term.[42] Corrections were made for the variation of the steady-state velocity with the inhibitor concentrations using eqs 3b and 3c as described earlier by Morrison and Walsh.[39]

$$v_s = \frac{k_7 SQ}{2(K_m + S)} \qquad (3b)$$

$$Q = [(K_i' + I_t - E_t) + 4K_i' E_t]^{1/2} - (K_i' + I_t - E_t) \qquad (3c)$$

where $K_i' = K_i^*(1 + S/K_m)$, I_t and E_t are the total inhibitor and enzyme concentrations, respectively. k_7 is the rate constant of the product formation

$$E + S \underset{k_2}{\overset{k_1}{\leftrightarrow}} ES \xrightarrow{k_7} E + P$$

The relationship between K_i, k_5, k_6, and k_{obs} is described by eq 4.

$$k_{obs} = k_6 + k_5\left(\frac{\frac{1}{K_i}}{1 + \left(\frac{[S]}{K_m}\right) + \left(\frac{[I]}{K_i}\right)}\right) \qquad (4)$$

The overall inhibition constant K_i^* is calculated by eq 5.

$$K_i^* = K_i \times \left(\frac{k_6}{(k_5 + k_6)}\right) \qquad (5)$$

Fluorescence Analysis of Triclosan Binding in the Presence of Tea Catechins and Polyphenols. Fluorescence analysis of triclosan binding was done as mentioned elsewhere[14] using a JobinYvon Horiba fluorimeter. The excitation and emission monochromator slit widths were adjusted at 3 nm. All the reactions were performed in 3 mL quartz cuvettes with constant stirring at 25 °C. Samples were excited at 295 nm, and emission was recorded between 300 to 500 nm. Change in the fluorescence intensity at the emission maximum of PfENR (340 nm) was then used for the studies of triclosan binding.

For the binding studies, 5 μM PfENR was incubated with different flavonoids at their saturating concentrations in 20 mM Tris and 150 mM NaCl, pH 7.4. The PfENR−catechin complex was titrated with increasing concentrations of triclosan from 0 to 30 μM. The difference in fluorescence intensity upon triclosan binding was analyzed using the following equations[43] to calculate the K_i value of triclosan.

$$F_0 - F = \frac{\Delta F_{max}}{1 + \left(\frac{K_i}{[I]}\right)} \qquad (6)$$

where $F_0 - F$ is the rapid fluorescence change, ΔF_{max} is maximum change in fluorescence, K_i is dissociation constant, and $[I]$ is the inhibitor concentration.

The onset of inhibition was calculated from the time course of fluorescence quenching at 340 nm after adding triclosan to the PfENR−catechin solution for 20 min. For tight-binding inhibitors, k_6 can be considered negligible at the early onset of inhibition, so k_5 can be directly calculated from the following equation,[43]

$$k_{obs} = \frac{k_5[I]}{\{K_i + [I]\}} \qquad (7)$$

where k_{obs} is the rate constant for the loss of fluorescence.

The inner filter effect was corrected by using the following equation,[44]

$$F_c = F_{anti} \log [(A_{ex} + A_{em})/2] \qquad (8)$$

where F_c is the corrected fluorescence and F is the measured one, and A_{ex} and A_{em} are the absorbance of the reaction solution at the excitation and emission wavelengths, respectively.

Docking of Inhibitors with *P. falciparum* and *E. coli* ENRs. All the docking simulations were done using AutoDock 3.05[45] and MOE [Molecular Operating Environment].[46]

Preparation of the Receptor and Ligand Molecules. The crystal structures of PfENR (PDB Code: 1NHG) and EcFabI (PDB Code: 1QSG) submitted to PDB (www.rcsb.org) by Perozzo et al.,[41] and Stewart et al.,[47] respectively, were used for docking studies. The structure coordinates were converted into mol2 format with MMFF94 charges assigned using the MOE suite of programs.[46] The molto2pdbqs utility (provided with AutoDock program) was used to prepare the input receptor file containing fragmental volume and solvation parameters. Inhibitors were also built using MOE and energy-minimized with MMFF94 charges. The AutoTors utility [provided with AutoDock program] was used to define torsion angles in the ligands prior to docking.

Docking Simulations. Grid maps for docking simulations were generated with 80 grid points (with 0.375 Å spacing) in x, y, and z directions centered in the active site using the AutoGrid utility of AutoDock program. Lennard−Jones parameters 12−10 and 12−6 (supplied with the program package) were used for modeling H-bonds and van der Waals interactions, respectively. The distance-dependent dielectric permittivity of Mehler and Solmajer[48] was used in the calculation of the electrostatic grid maps. The Lamarckian genetic algorithm (LGA) with the pseudo-Solis and Wets modification (LGA/pSW) method was used with default parameters except the "maximum number of energy evaluations" which was increased to 2.5 million from 250 thousand. Hundred independent runs were conducted for each inhibitor.

Modeling of the Ternary Complex. The ternary complex PfENR−EGCG−TCL was achieved by first docking the tea catechins with PfENR to generate the binary complex and then docking triclosan to this binary complex. Briefly, the top-ranked conformation of the biggest cluster in the set of 100 runs of EGCG docking with PfENR was chosen. Now this binary complex was prepared as the receptor (as described above), and triclosan was docked using AutoDock with this binary complex, using the same protocol as mentioned above. Since the receptor remains rigid during the docking simulation by AutoDock, the docked complexes were energy-minimized to 0.1 kcal/mol, keeping the receptor and the ligand flexible. This accounts for the minor structural changes that take place in the receptor as well as in the ligand. The ligand−receptor interactions were calculated using LPC/CSU Server [http://ligin.weizmann.ac.il/cgi-bin/lpccsu/LpcCsu.cgi].

Acknowledgment. This work was supported by grants from the Department of Biotechnology, Government of India, to N.S. and A.S. A.S. is also a recipient of a Centre of Excellence grant from the Department of Biotechnology, Government of India. S.K.S. and G.K. are senior research fellows supported by CSIR, Government of India.

Supporting Information Available: Kinetic plots of flavonoids other than EGCG (K_i, progress curves, k_{obs}, v_s [triclosan], k_6, and fluorescence titration curves) along with detailed docking simulation figures showing the spread of all 100 conformations of the docked

ligand. This material is available free of charge via the Internet at http:// pubs.acs.org.

References

(1) *The World Health Report 1999*; WHO: Geneva, pp 49−63.
(2) Surolia, N.; Surolia, A. Triclosan offers protection against blood stages of malaria by inhibiting enoyl-ACP reductase of *Plasmodium falciparum*. *Nat. Med.* **2001**, *7*, 167−173.
(3) Wiesner, J.; Seeber, F. The plastid-derived organelle of protozoan human parasites as a target of established and emerging drugs. *Expert Opin. Ther. Targets* **2005**, *9*, 23−44.
(4) Smith, S.; Witkowski, A.; Joshi, A. K. Structural and functional organization of the animal fatty acid synthase. *Prog. Lipid Res.* **2003**, *42*, 289−317.
(5) Rock, C. O.; Cronan, J. E. *Escherichia coli* as a model for the regulation of dissociable (type II) fatty acid biosynthesis. *Biochim. Biophys. Acta* **1996**, *1302*, 1−16.
(6) Heath, R. J.; Rock, C. O. Fatty acid biosynthesis as a target for novel antibacterials. *Curr. Opin. Investig. Drugs* **2004**, *5*, 46−53.
(7) Surolia, A.; Ramya, T. N. C.; Ramya, V.; Surolia, N. 'FAS't inhibition of malaria. *Biochem. J.* **2004**, *383*, 401−412.
(8) Sharma, S. K.; Kapoor, M.; Ramya, T. N. C.; Kumar, G.; Kumar, S.; Modak, R.; Sharma, S.; Surolia, N.; Surolia, A. Identification, characterization, and inhibition of *Plasmodium falciparum* beta-hydroxyacyl-acyl carrier protein dehydratase [FabZ]. *J. Biol. Chem.* **2003**, *278*, 45661−45671.
(9) Ralph, S. A.; Van Dooren, G. G.; Waller, R. F.; Crawford, A. F.; Fraunholz, M. J.; Foth, B. J.; Tonkin, C. J.; Roos, D. S.; McFadden, G. I. Metabolic maps and functions of the *Plasmodium falciparum* apicoplast. *Nat. Rev. Microbiol.* **2004**, *2*, 203−216.
(10) Waller, R. F.; Reed, M. B.; Cowman, A. F.; McFadden, G. I. Protein trafficking to the plastid of *Plasmodium falciparum* is via the secretory pathway. *EMBO J.* **2000**, *19*, 1794−1802.
(11) Heath, R. J.; Rock, C. O. Enoyl-acyl carrier protein reductase (*fabI*) plays a determinant role in completing cycles of fatty acid elongation in *Escherichia coli*. *J. Biol. Chem.* **1995**, *270*, 26538−26542.
(12) Zhang, Y. M.; Lu, Y. J.; Rock, C. O. The reductase steps of the type II fatty acid synthase as antimicrobial targets. *Lipids* **2004**, *39*, 1055−60.
(13) Kapoor, M.; Dar, M. J.; Surolia, A.; Surolia, N. Kinetic determination of the interaction of Enoyl-ACP Reductase from *Plasmodium falciparum* with its substrates and inhibitors. *Biochem. Biophys. Res. Commun.* **2001**, *289*, 832−837.
(14) Kapoor, M.; Reddy, C. C.; Krishnasastry, M. V.; Surolia, N.; Surolia, A. Slow-tight-binding inhibition of enoyl-acyl carrier protein reductase from *Plasmodium falciparum* by triclosan. *Biochem. J.* **2004**, *381*, 719−24.
(15) Kapoor, M.; Mukhi, P. L.; Surolia, N.; Suguna, K.; Surolia, A. Kinetic and structural analysis of the increased affinity of enoyl-ACP (acyl-carrier protein) reductase for triclosan in the presence of NAD^+. *Biochem. J.* **2004**, *381*, 725−733.
(16) Kapoor, M.; Gopalakrishnapai, J.; Surolia, N.; Surolia, A. Mutational analysis of the triclosan-binding region of enoyl-ACP(Acyl Carrier Protein) reductase from *Plasmodium falciparum*. *Biochem. J.* **2004**, *381*, 735−741.
(17) Pidugu, L. S.; Kapoor, M.; Surolia, N.; Surolia, A.; Suguna, K. Structural basis for the variation in triclosan affinity to Enoyl Reductases. *J. Mol. Biol.* **2004**, *343*, 147−155.
(18) Taylor, N. in *Green Tea, The Natural Secret for a Healthier Life*; Kensington Publishing Corp.: New York, NY, 1998.
(19) Cooper, R.; Morré, D. J.; Morré, D. M. Medicinal Benefits of Green Tea: Part II. Review of Anticancer Properties. *J. Alternat. Complement. Med.* **2005**, *11*, 639−652.
(20) Yang, C. S.; Wang, Z. Y. Tea and Cancer. *J. Natl. Cancer Inst.* **1993**, *85*, 1038−1049.
(21) Bastianetto, S.; Yao, Z. X.; Papadopoulos, V.; Quirion, R. Neuroprotective effects of green and black teas and their catechin gallate esters against beta-amyloid-induced toxicity. *Eur. J. Neurosci.* **2006**, *23*, 55−64.
(22) Dorchies, O. M.; Wagner, S.; Vuadens, O.; Waldhauser, K.; Buetler, T. M.; Kucera, P.; Ruegg, U. T. Green tea extract and its major polyphenol (−)-epigallocatechin gallate improve muscle function in a mouse model for Duchenne muscular dystrophy. *Am. J. Physiol. Cell. Physiol.* **2006**, *290*, 616−25.
(23) Cao, Y.; Cao, R. Angiogenesis inhibited by drinking tea. *Nature* **1999**, *398*, 381.
(24) Yamakawa, S.; Asai, T.; Uchida, T.; Matsukawa, M.; Akizawa, T.; Oku, N. Epigallocatechin gallate inhibits membrane-type 1 matrix metalloproteinase, MT1-MMP, and tumor angiogenesis. *Cancer Lett.* **2004**, *210*, 47−55.
(25) Kitashirakawa, O.; Kyoto, S. Inhibition of human matrix metalloproteinase-7 (MMP-7), an enzyme involved in cancer metastasis, by catechins, *Foods Food Ingred. J. Jpn.* **2003**, *208*, 975−979.
(26) Tillekeratne, L. M. V.; Sherette, A.; Grossman, P.; Hupe, L.; Hupe, D.; Hudson, R. A. Simplified catechin-gallate inhibitors of HIV-1 reverse transcriptase. *Bioorg. Med. Chem. Lett.* **2001**, *11*, 2763−2767.
(27) Seeram, N. P.; Zhang, Y.; Nair, M. G. Inhibition of proliferation of human cancer cells and cyclooxygenase enzymes by anthocyanidins and catechins. *Nutr. Cancer* **2003**, *46*, 101−106.
(28) Naasani, I.; Seimiya, H.; Tsuruo, T. Telomerase inhibition, telomere shortening, and senescence of cancer cells by tea catechins. *Biochem. Biophys. Res. Commun.* **1998**, *249*, 391−396.
(29) Seki, A. T.; Noguchi, H.; Kashiwada, Y. Galloyl esters from rhubarb are potent inhibitors of squalene epoxidase, a key enzyme in cholesterol biosynthesis. *Planta Med.* **2000**, *66*, 753−756.
(30) Wang, X.; Tian, W. Green tea epigallocatechin gallate: a natural inhibitor of fatty-acid synthase. *Biochem. Biophys. Res. Commun.* **2001**, *288*, 1200−1206.
(31) Li, B. H.; Tian, W. X. Inhibitory effects of flavonoids on animal fatty acid synthase. *J. Biochem.* **2004**, *135*, 85−91.
(32) Ghosh, K. S.; Maiti, T. S.; Dasgupta, S. Green tea polyphenols as inhibitors of ribonuclease A. *Biochem. Biophys. Res. Commun.* **2004**, *325*, 807−811.
(33) Zhang, Y. M.; Rock, C. O. Evaluation of epigallocatechin gallate and related plant polyphenols as inhibitors of the FabG and FabI reductases of bacterial type II fatty-acid synthase. *J. Biol. Chem.* **2004**, *279*, 30994−1001.
(34) Tasdemir, D.; Lack, G.; Burn, R.; Ruedi, P.; Scapozza, L.; Perozzo, R. Inhibition of *Plasmodium falciparum* fatty acid biosynthesis: Evaluation of FabG, FabZ, and FabI as drug targets for flavonoids. *J. Med. Chem.* **2006**, *49*, 3345−3353.
(35) Dixon, M. The Graphical Determination of K_m and K_i. *Biochem. J.* **1972**, *129*, 197−202.
(36) Ward, W. H. J.; Holdgate, G. A.; Rowsell, S.; McLean, E. G.; Pauptit, R. A.; Clayton, E.; Nichols, W. W.; Colls, J. G.; Minshull, C. A.; Jude, D. A.; Mistry, A.; Timms, D.; Camble, R.; Hales, N. J.; Britton, C. J.; Taylor, I. W. F. Kinetic and Structural Characteristics of the Inhibition of Enoyl (Acyl Carrier Protein) Reductase by Triclosan. *Biochemistry* **1999**, *38*, 12514 − 12525.
(37) Heath, R. J.; Rubin, J. R.; Holland, D. R.; Zhang, E.; Snows, M. E.; Rock, C. O. Mechanism of triclosan inhibition of bacterial fatty acid synthesis. *J. Biol. Chem.* **1999**, *274*, 11110−11114.
(38) Scatchard, G. The attraction of proteins for small molecules and ions. *Ann. N. Y. Acad. Sci.* **1949**, *51*, 660.
(39) Morrison, J. F.; Walsh, C. T. The behavior and significance of slow-binding enzyme inhibitors. *Adv. Enzymol. Relat. Areas Mol. Biol.* **1988**, *61*, 201−301.
(40) Morrison, J. F. The slow binding and slow-tight binding inhibition of enzyme catalyzed reactions. *Trends Biochem. Sci.* **1982**, *7*, 102−105.
(41) Perozzo, R.; Kuo, M.; Sidhu, A. S.; Valiyaveettil, J. T.; Bittman, R.; Jacobs, W. R., Jr.; Fidock, D. A.; Sacchettini, J. C. Structural Elucidation of the Specificity of the Antibacterial Agent Triclosan for Malarial Enoyl ACP Reductase. *J. Biol. Chem.* **2002**, *277*, 13106−13114.
(42) McClerren, A. L.; Endsley, S.; Bowman, J. L.; Anderson, N. H.; Guan, Z.; Rudolph, J.; Raetz, C. R. H. A slow, tight-binding inhibitor of the Zinc-dependent deacetylase LpxC of lipid. A biosynthesis with antibiotic activity comparable to Ciprofloxacin. *Biochemistry* **2005**, *44*, 16474−16583.
(43) Houtzager, V.; Oullet, M.; Flagueyret, J. −P.; Passmore,l. A.; Bayly, C.; Percival, M. D. Inhibitor-induced changes in the intrinsic fluorescence of human cyclooxygenase-2. *Biochemistry* **1996**, *35*, 10974−10984.
(44) Lakowicz, J. R. *Principles of Fluorescence Spectroscopy*; Plenum Press: New York, 1983; pp 180−195.
(45) Morris, G. M.; Goodsell, D. S.; Halliday, R. S.; Huey, R.; Hart, W. E.; Belew, R. K.; and Olson, A. J. Automated Docking Using a Lamarckian Genetic Algorithm and Empirical Binding Free Energy Function. *J. Comput. Chem.* **1998**, *19*, 1639−1662.
(46) Molecular Operating Environment [MOE 2001.07], Chemical Computing Group Inc.,1255 University St., Suite 1600, Montreal, Quebec, Canada, H3B 3X3.
(47) Stewart, M. J.; Parikh, S.; Xiao, G.; Tonge, P. J.; Kisker, C. Structural Basis and Mechanism of Enoyl Reductase Inhibition by Triclosan. *J. Mol. Biol.* **1999**, *290*, 859−865.
(48) Mehler, E. L.; Solmajer, T. Electrostatic effects in proteins: comparison of dielectric and charge models. *Protein Eng.* **1991**, *4*, 903−910.

JM061154D